Ultra-wide-band Circularly Polarized Mushroom-shaped Dielectric Resonator Antenna for 5G and sub-6 GHz Applications

Ultra-wide-band Circularly Polarized Mushroom-shaped Dielectric Resonator Antenna for 5G and sub-6 GHz Applications

Sumer Singh Singhwal, Ladislau Matekovits*, *Senior Member, IEEE,*

***Abstract*—In this dissemination, a mushroom shaped ultra-wideband circularly polarized Dielectric Resonator Antenna (DRA) is proposed for lower 5G band and sub-6 GHz applications. The proposed DRA is excited by two orthogonal conformal probes and fed by a simple L shape microstrip feed network. The DRA exhibits wide impedance bandwidth of approximately 34.5% (3.5-5.1 GHz) with S_{11} better than -10 dB and wide circular polarization bandwidth of 33% (3.55-5 GHz) with axial-ratio less than 3 dB in broadside direction. Mushroom-shaped DRA has a peak gain of 6.5 dB and an average gain throughout the operating band is 5.5 dB. Simulated results of the DRA are in good agreements with measured results of fabricated prototype. This DRA is a strong candidate for the sub-6 GHz and 5G band applications.**

***Index Terms*—5G, circular polarization, DRA, mushroom-shaped, sub-6 GHz**

I. Introduction

Dielectric Resonator Antennas (DRA) are the preferred choice in the spurting field of wireless communications because of their plenty of advantages. Advantages of DRA include their small size, wide operating bandwidth, low losses, multiple excitation schemes and multiple design parameters. They display wide bandwidth because their radiation area is greater than microstrip patch antenna. DRAs have more degree of freedom to design such as length, width and height in rectangular DRA and radius and height in cylindrical DRA. They showcase low losses because of the absence of metallic boundary and surface. DRA can work in different modes depending upon type of feeding scheme used. Petosa et al. [1] explained that radiation efficiency of a DRA is substantially unaffected by the dielectric constant of DRA and low loss dielectric material with ($2 \leq \epsilon_r \leq 140$) can be used for the purpose of antenna. The motivation behind this study is to design a DRA for sub-6 GHz band with low dielectric constant material because recent DRAs are designed generally with high or medium permittivity material i.e. ($10 \leq \epsilon_r \leq 80$). In [2] Pan et al, compared performances of low permittivity DRA ($\epsilon_r = 5$) with medium permittivity DRA ($\epsilon_r = 10$) and concluded that a lower permittivity DRA is recommendable for achieving wide bandwidth but the size of DRA is also increased, and mode excitation in low permittivity DRA is also difficult in comparison with high permittivity DRA. In [3], Sun et al. use K9-glass a low dielectric constant material (ϵ_r=6.85) to make a dual-band dual-polarized cylindrical DRA. In [4] a FR4 material made DRA with circular microstrip feed network was proposed for microwave image sensing applications at 28 GHz.

In this paper, a new shape of DRA named Mushroom DRA (MDRA) is investigated which is the combination of cylindrical and hemispherical DRA and which radiate over large bandwidth. To achieve circular polarisation two orthogonal feeds are used. The antenna operates at 3-5 GHz frequency range. Impedance bandwidth (IBW) of the antenna is 34.5% having range 3.5-5.1 GHz. Axial Ratio BandWidth (ARBW) is 33% from 3.55-5 GHz. Peak gain at broadside direction and average gain throughout the operating band are 6.5 dB and 5.5dB respectively. Latest International Telecommunication Union documentation [5] suggests lower 5G bands for 5G communication are 3.5-5 GHz. Proposed MDRA operates precisely in this band with circular polarization throughout the operating band.

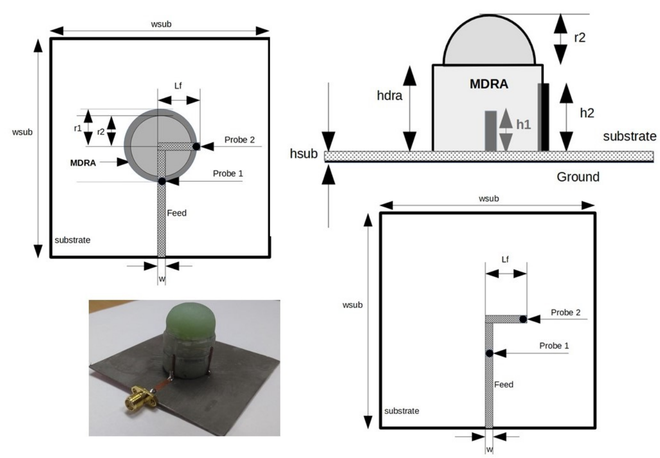

Fig. 1: Geometry of MDRA and fabricated prototype

II. Design and Operating Principle

A. Design Methodology

The geometry of the wideband circularly polarized MDRA is shown in Fig. 1 which has dimensional parameters given in Table-I. In this paper, DRA material is chosen with low

*Corresponding author email: ladislau.matekovits@polito.it

Department of Electronics and Telecommunications, Politecnico di Torino, 10129 Torino, Italy.

Istituto di Elettronica e di Ingegneria dell Informazione e delle Telecomunicazioni, National Research Council of Italy, 10129 Turin, Italy.

Department of Measurements and Optical Electronics, Politehnica University Timişoara, 300223 Timişoara, Romania

TABLE I
DESIGN PARAMETERS

Parameter	in mm	Parameter	in mm
wsub	72	hsub	0.8
hdra	20	w	2.4
h1	9	h2	15
r1	12	r2	11
Lf	14		

dielectric constant $\epsilon_{r,DRA}$=4.4, FR4 fiberglass epoxy. Albeit, formulas to determine radius and height of DRA are available for $\epsilon_r \geq 10$ [6], so these design relations cannot be applied here directly. However, the dimension of any dielectric resonator antenna is proportional inversely to $\sqrt{\epsilon_r}$ [3]. The inverse methodology adopted here, first finding the dimension of DRA for ϵ_r=10 using [6] and then rescaling dimension to the present case of ϵ_r=4.4 followed by fine-tuning of parameters using HFSS simulator. Design equation used in [6] for $HE_{11\delta}$ mode.

$$f_0 = \frac{c \times 6.324}{2\pi a\sqrt{\epsilon_{DRA}+2}}\left[0.27 + 0.36\left(\frac{a}{2H}\right) + 0.02\left(\frac{a}{2H}\right)^2\right] \quad (1)$$

where a, H and ϵ_{DRA} are the radius, height, and dielectric constant of the DRA respectively and c is the velocity of light in vacuum. The substrate is RT/Duroid5870 with a relative dielectric constant of 2.33, area of 72×72 mm^2 and height of 0.8 mm. Perpendicular feed configurations with width 2.4 mm and heights 9 mm and 15 mm, respectively has been adopted to excite MDRA orthogonally, so that our proposed antenna produces circular polarization.

Design methodology of antenna involves two steps: first step is to design a cylindrical DRA (CDRA) with a height hdra=20 mm; second step is placing a hemisphere of radius r2=11 mm on the top CDRA to improve its results. The final structure after placing hemisphere on the top of the cylinder resembles the mushroom shape so-called MDRA. Comparison of impedance bandwidth, Gain and AR bandwidth between step1 and step2, are shown in Fig. 2. Antenna parameters in case of step 2(MDRA) have been improved effectively without any change in the resonance frequency. Therefore, a hemisphere is coupled with the CDRA in such that resonance frequency remains the same but circular polarization increases due to the increase in surface area, in the formed MDRA. Circular polarization can be achieved in the MDRA by adopting hybrid feeding configuration, which is a combination of microstrip feed line and probe feed. This hybrid feeding consists of a L-shape microstrip feed line network with two orthogonal, conformal, engraved probes, as shown in Fig. 2(a). So, the proposed MDRA is excited by two conformal probes, which are engraved on the MDRA with 0.25 mm insert depth and placed at the orthogonal position with one another. Here phase quadrature condition is obtained between orthogonal hybrid modes ($HE^x_{11\delta}$ and $HE^y_{11\delta}$) by modifying the corresponding probe lengths.

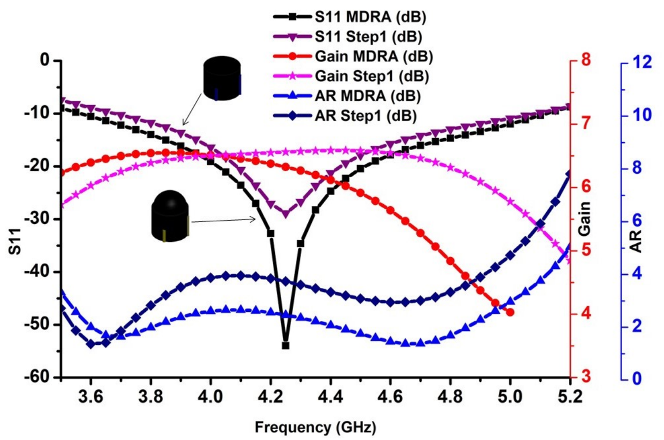

Fig. 2: Comparison between S_{11}, Gain and Axial Ratio Bandwidth of CDRA (step-1) and MDRA (step-2)

B. Operational Principle

The operation of MDRA is explained in three steps. In step one, MDRA is excited by single probe-1 such that $HE^x_{11\delta}$ mode dominates but circular polarization. In the second step, MDRA is excited by single probe-2 such that $HE^y_{11\delta}$ mode dominates. In the third step, MDRA is excited by both the probes (probe-1 and probe-2) which results in merging of both the $HE^x_{11\delta}$ and $HE^y_{11\delta}$ modes and producing circular polarization. Heights of probe-1 and probe-2 have been optimized to attain phase quadrature condition between two orthogonal hybrid modes, to achieve circular polarization. Two dips at 3.7 GHz and 4.6 GHz in AR plot shown in Fig.2 confirm the presence of both the modes. Figure 3 illustrates the S_{11} parameters of all three operational steps corresponding to MDRA excited by probe-1, probe-2 and both the probes, respectively. Electric field inside MDRA corresponding to all three steps explained above is shown in Fig. 3.

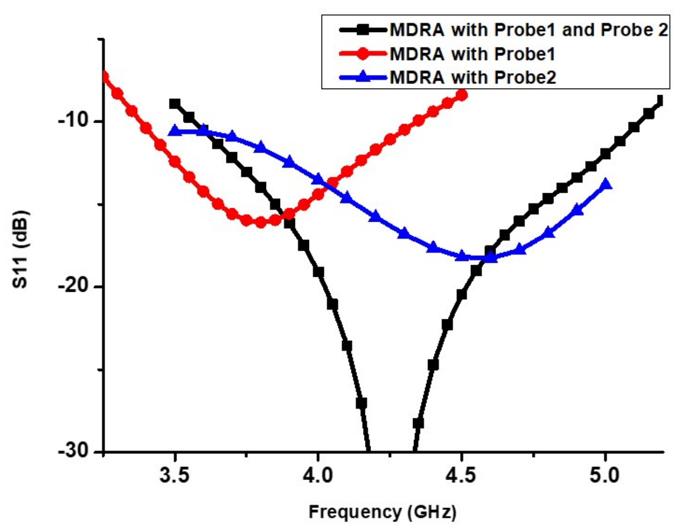

Fig. 3: Operational steps: S_{11} comparison and E Field of MDRA with Probe-1, Probe-2 and both probes respectively

III. Results and Discussion

For the verification of the simulated results, a prototype of the proposed DRA has been fabricated, as shown in Fig. 1. Figure 4 shows the comparison between simulated and measured reflection coefficient and gain. Measured results are in approximate agreement with simulated results because of manual fabrication of MDRA. Figure 5 shows the comparison between simulated and measured AR in broadside direction ($\theta = 0, \phi = 0$) and simulated radiation efficiency. It is observed from Fig. 5 that radiation efficiency maximizes up to 66% at the center frequency. This moderate radiation efficiency is due to lossy FR4 material used in the construction of DRA. IBW is 34% (3.5-5.1 GHz) whereas ARBW is almost covering the complete operating band (3.55-5 GHz). Peak gain in the broadside direction is 6.5 dB whereas average gain is around 5.5 dB throughout the operating band.

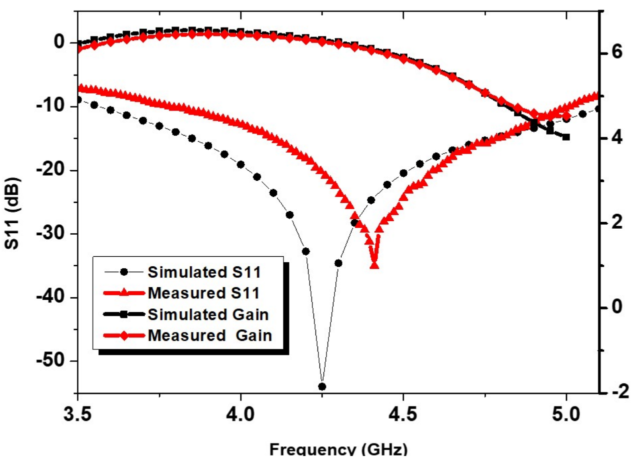

Fig. 4: Simulated and measured S_{11} parameter and Gain of proposed DRA

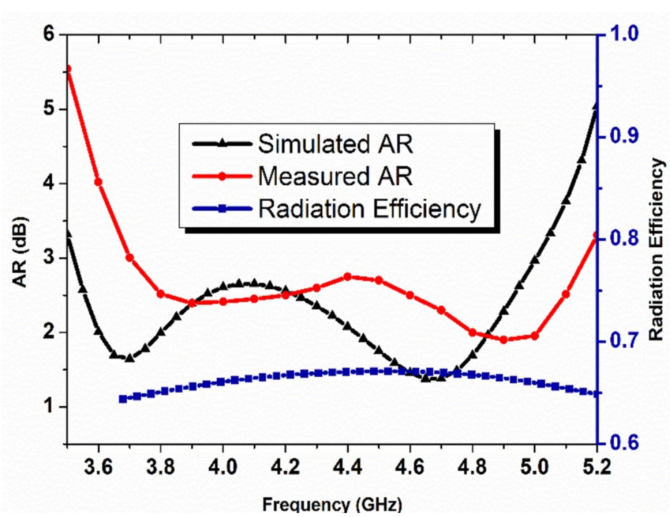

Fig. 5: Simulated and measured ARBW and simulated radiation efficiency of proposed DRA

The radiation pattern at two band edge frequencies (3.75 GHz, 4.6 GHz) in the operating frequency range are shown in Fig. 6. It depicts uniformity in radiation pattern at these frequencies which confirm uniform behavior of radiation pattern throughout the operating frequency band. It shows E-plane and H-plane co-polarization and cross-polarization field radiation pattern at 3.75 GHz and 4.6 GHz frequencies. It is also observed that for both E-plane and H-plane measured Co-Pol fields are greater than Cross-Pol fields by $\approx$ 20 dB in the broadside direction ($\theta = 0, \phi = 0$).

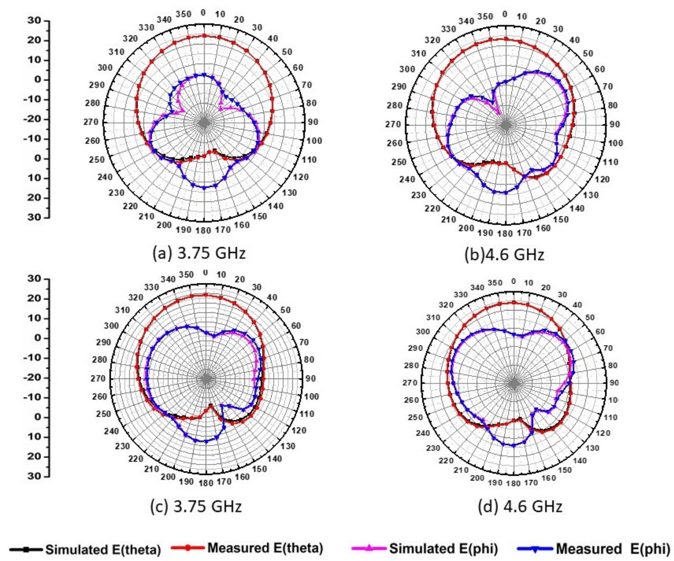

Fig. 6: Radiation pattern of MDRA in E-plane (a,b) and H-plane (c,d) at frequencies 3.75 GHz, 4.6 GHz

Table II represents other antenna metrics such as half power beamwidth (HPBW), front to back ratio (F/B), side lobe level (SLL), first null beamwidth (FNBW) for two band edge frequencies. Radiation characteristics were examined at other frequencies of the operating band and found good across complete operating band. Table-III shows a comparison of our proposed MDRA with recently published DRA designs. It is found that proposed antenna design is simple and performance is better in all departments when compared to other recent designs. Electric field distribution inside MDRA for different phase angles at frequency 4.3 GHz is illustrated in Fig. 7. It confirms presence of the LHCP field in the MDRA.

TABLE II
Antenna Radiation parameters

Frequency	HPBW	F/B	SLL	FNBW
3.75 GHz	80°	11.1 dB	11.1 dB	360°
4.6 GHz	110°	11.3 dB	9.9 dB	260°

IV. Conclusion

In this paper, a mushroom-shaped DRA is constructed with low dielectric constant material which exhibits 34.5% impedance bandwidth and 33% axial ratio bandwidth with peak gain of 6.5 dB. The proposed design is novel and simple in construction without any cuts and slots. An L shape microstrip feed line network with two orthogonal, conformal, engraved probes are used to excite hybrid modes in MDRA.

TABLE III
COMPARISON WITH RECENTLY PUBLISHED DESIGNS

Ref.	DRA shape	DRA Volume (mm^3)	IBW (%)	ARBW (%)	Gain (dBi)	Frequency (GHz)	Feed Method
[7]	Trapezoidal	16800	34	21	8.6	3.2	Aperture Coupled
[8]	Cylindrical	9852	10	6.4	7.7	3.46	Probe
[9]	Cylindrical	776	43.3	42.8	3	6	Quadrature Feed Network
[10]	Cylindrical	3180	5.8	3.4	2.7	2.4	Off-centered microstrip line
[11]	Rectangular	5832	35	20.6	1.5	3.29	Question mark shaped microtrip feed
[12]	Triangular	623	12.37, 4.8	1.6, 1.8	2.15, 3.69	7.5, 8.7	Probe
[13]	Rectangular	5832	12, 9	4, 0	3, 5	2.4, 3.3	Cross shape slot coupled feed
Proposed	Mushroom	9047	34.5	33	6.5	4.6	L-shape microstrip line

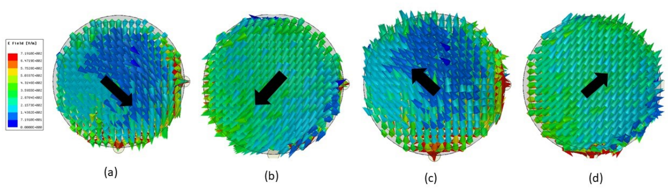

Fig. 7: Electric Field distribution in MDRA at (a) 0 (b) 90° (c) 180° (d) 270° time phase at 4.3 GHz

Advantages of the proposed antenna are ease of design and complete overlapping of impedance bandwidth and ARBW with good gain. ITU documentation [5] suggests that the 3.5-5 GHz band is to be proposed for lower 5G band communication. Proposed antenna is a good candidate for 5G communication in this band and other sub-6 GHz applications.

REFERENCES

[1] A. Petosa and A. Ittipiboon, "Dielectric Resonator Antennas: A Historical Review and the Current State of the Art," in *IEEE Antennas and Propagation Magazine*, vol. 52, no. 5, pp. 91-116, Oct. 2010, doi: 10.1109/MAP.2010.5687510.

[2] Y. Pan, K. W. Leung and K. Luk, "Design of the Millimeter-wave Rectangular Dielectric Resonator Antenna Using a Higher-Order Mode," in *IEEE Transactions on Antennas and Propagation*, vol. 59, no. 8, pp. 2780-2788, Aug. 2011, doi: 10.1109/TAP.2011.2158962.

[3] Y. X. Sun and K. W. Leung, "Dual-Band and Wideband Dual-Polarized Cylindrical Dielectric Resonator Antennas," in *IEEE Antennas and Wireless Propagation Letters*, vol. 12, pp. 384-387, 2013, doi: 10.1109/LAWP.2013.2251993.

[4] S. S. Singhwal, B. K. Kanujia, A. Singh, J. Kishor,"Novel circularly polarized dielectric resonator antenna for microwave image sensing application", *Microwave and Optical Technology Letters*, vol. 29, no. 9, Sept. 2019.

[5] ITU document on 5G spectrum allocation $https://www.itu.int/en/ITU-D/Regulatory-Market/Documents/Events2019/Togo/5G-Ws/Ses4_{joaquin}{_spectrum}-5G.pdf$ last accessed on 25-08-2021

[6] R. K. Mongia,P. Bhartia,"Dielectric resonator antennas—A review and general design relations for resonant frequency and bandwidth", in *Int. J. RF Microw Millim. Comput.-Aided Eng.*, Vol. 4, no. 3, pp. 230–247, 1994.

[7] Y. Pan and K. W. Leung, "Wideband Circularly Polarized Trapezoidal Dielectric Resonator Antenna," in *IEEE Antennas and Wireless Propagation Letters*, vol. 9, pp. 588-591, 2010, doi: 10.1109/LAWP.2010.2053910.

[8] A. Motevasselian, A. Ellgardt and B. L. G. Jonsson, "A Circularly Polarized Cylindrical Dielectric Resonator Antenna Using a Helical Exciter," in *IEEE Transactions on Antennas and Propagation*, vol. 61, no. 3, pp. 1439-1443, March 2013, doi: 10.1109/TAP.2012.2229954.

[9] R. Y. Sun, Q. H. Chen,"Quadrature feed wideband circularly polarized cylindrical dielectric resonator antenna", in *J. Electromagn. Waves Appl.*, vol. 28, no.8, pp. 1011-1017, 2014.

[10] C. Lin and J. Sun, "Circularly Polarized Dielectric Resonator Antenna Fed by Off-Centered Microstrip Line for 2.4-GHz ISM Band Applications," in *IEEE Antennas and Wireless Propagation Letters*, vol. 14, pp. 947-949, Dec. 2015, doi: 10.1109/LAWP.2014.2388075.

[11] R. Kumar and R. K. Chaudhary, "A Wideband Circularly Polarized Cubic Dielectric Resonator Antenna Excited With Modified Microstrip Feed," in *IEEE Antennas and Wireless Propagation Letters*, vol. 15, pp. 1285-1288, 2016, doi: 10.1109/LAWP.2015.2504840.

[12] S. K. K. Dash, T. Khan and B. K. Kanaujia, "Circularly Polarized Dual Facet Spiral Fed Compact Triangular Dielectric Resonator Antenna for Sensing Applications," in *IEEE Sensors Letters*, vol. 2, no. 1, pp. 1-4, March 2018, Art no. 3500404, doi: 10.1109/LSENS.2018.2795017.

[13] R. Kumar, R. K. Chaudhary,"A dual-band dual-polarized cubical DRA coupled with new modified cross-shaped slot for ISM (2.4 GHz) and Wi-MAX (3.3-3.6 GHz) band applications",in *International Journal of RF Microwave Computer Aided Eng.*, Vol. 29, no.1, 2019.